Article

Common and Divergent Structural Features of a Series of Corticotropin Releasing Factor-Related Peptides

Christy Rani R. Grace, Marilyn H. Perrin, Jeffrey P. Cantle, Wylie W. Vale, Jean E. Rivier, and Roland Riek

J. Am. Chem. Soc., **2007**, 129 (51), 16102-16114 • DOI: 10.1021/ja0760933

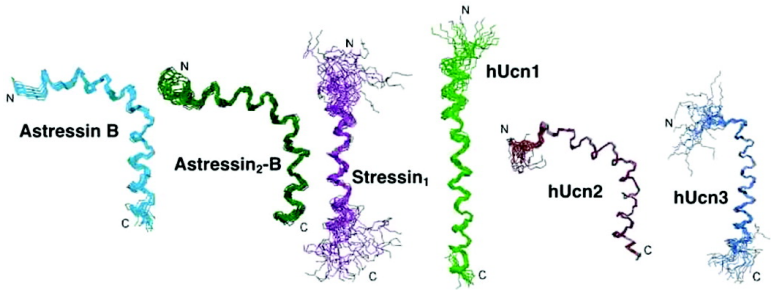

More About This Article

Additional resources and features associated with this article are available within the HTML version:

- Supporting Information
- Access to high resolution figures
- Links to articles and content related to this article
- Copyright permission to reproduce figures and/or text from this article

View the Full Text HTML

J|A|C|S
ARTICLES
Published on Web 12/06/2007

Common and Divergent Structural Features of a Series of Corticotropin Releasing Factor-Related Peptides

Christy Rani R. Grace,[†] Marilyn H. Perrin,[‡] Jeffrey P. Cantle,[‡] Wylie W. Vale,[‡] Jean E. Rivier,*[,‡] and Roland Riek*[,†]

Structural Biology Laboratory and The Clayton Foundation Laboratories for Peptide Biology, The Salk Institute for Biological Studies, 10010 North Torrey Pines Road, La Jolla, California 92037

Received August 16, 2007; E-mail: riek@salk.edu

Abstract: Members of the corticoliberin family include the corticotropin releasing factors (CRFs), sauvagine, the urotensins, and urocortin 1 (Ucn1), which bind to both the CRF receptors CRF-R1 and CRF-R2, and the urocortins 2 (Ucn2) and 3 (Ucn3), which are selective agonists of CRF-R2. Structure activity relationship studies led to several potent and long-acting analogues with selective binding to either one of the receptors. NMR structures of six ligands of this family (the antagonists astressin B and astressin$_2$-B, the agonists stressin$_1$, and the natural ligands human Ucn1, Ucn2, and Ucn3) were determined in DMSO. These six peptides show differences in binding affinities, receptor-selectivity, and NMR structure. Overall, their backbones are α-helical, with a small kink or a turn around residues 25−27, resulting in a helix−loop−helix motif. The C-terminal helices are of amphipathic nature, whereas the N-terminal helices vary in their amphipathicity. The C-terminal helices thereby assume a conformation very similar to that of astressin bound to the ECD1 of CRF-R2 recently reported by our group.[1] On the basis of an analysis of the observed 3D structures and relative potencies of [Ala]-substituted analogues, it is proposed that both helices could play a crucial role in receptor binding and selectivity. In conclusion, the C-terminal helices may interact along their hydrophobic faces with the ECD1, whereas the entire N-terminal helical surface may be involved in receptor activation. On the basis of the common and divergent features observed in the 3D structures of these ligands, multiple binding models are proposed that may explain their plurality of actions.

1. Introduction

Corticotropin releasing factor (CRF) is a 41-amino acid polypeptide[2] belonging to the corticoliberin peptide family, whose members are the CRFs and the CRF-like peptides, urocortins 1−3 (Ucn),[3] the fish peptides, urotensins I,[4] and the frog skin peptide, sauvagine (Svg).[5] CRF-like peptides are present in the cardiovascular, gastrointestinal, reproductive, immune, and central nervous systems and the skin and account for a wide range of stress-related responses. They exert their biological actions by binding to either one of two seven transmembrane helical receptors designated CRF-R1 and CRF-R2, belonging to the family B1 G-protein-coupled receptors (GPCR). The CRF-like peptide hormones activate these receptors by a two-step binding process, as has been proposed for the B1 family receptors and their respective ligands.[6−14] The C-terminal segment of the CRF-like ligands interacts in a helical conformation with the ECD1 of the CRF receptor mainly via hydrophobic interactions.[1,15] Formation of this complex orients the ligand and the receptor, enabling receptor activation through interaction between the serpentine segment of the receptor and the N-terminal segment of the ligand.[14,16] This hypothesis is based on the observation: (1) that truncation of the first eight N-terminal residues results in an antagonist[17] and (2) that the first 16 N-terminal residues of the ligand suffice to activate the receptor.[16] Furthermore, C-terminal truncations or des-amidation of the ligands result in a drastic decrease in their potencies.[2]

[†] Structural Biology Laboratory.
[‡] The Clayton Foundation Laboratories for Peptide Biology.

(1) Grace, C. R. R.; Perrin, M.; Gulyas, J.; DiGruccio, M.; Cantle, J. P.; Rivier, J.; Vale, W.; Riek, R. *Proc. Natl. Acad. Sci. U.S.A.* **2007**, *104*, 4858−4863.
(2) Vale, W.; Spiess, J.; Rivier, C.; Rivier, J. *Science* **1981**, *213*, 1394−1397.
(3) Vaughan, J. M.; Donaldson, C.; Bittencourt, J.; Perrin, M. H.; Lewis, K.; Sutton, S.; Chan, R.; Turnbull, A.; Lovejoy, D.; Rivier, C.; Rivier, J.; Sawchenko, P. E.; Vale, W. *Nature* **1995**, *378*, 287−292.
(4) Lederis, K.; Vale, W. W.; Rivier, J. E.; MacCannell, K. L.; McMaster, D.; Kobayashi, Y.; Suess, U.; Lawrence, J. *Proc. West. Pharmacol. Soc.* **1982**, *25*, 223−227.
(5) Erspamer, V.; Melchiorri, P. *Trends Pharmacol. Sci.* **1980**, *20*, 391−395.
(6) Feyen, J. H.; Cardinaux, F.; Gamse, R.; Bruns, C.; Azria, M.; Trechsel, U. *Biochem. Biophys. Res. Commun.* **1992**, *187*, 8−13.
(7) Coy, D. H.; Murphy, W. A.; Sueiras-Diaz, J.; Coy, E. J.; Lance, V. A. *J. Med. Chem.* **1985**, *28*, 181−185.
(8) Coy, D. H.; Murphy, W. A.; Lance, V. A.; Heiman, M. L. *J. Med. Chem.* **1987**, *30*, 219−222.
(9) Rittel, W.; Maier, R.; Brugger, M.; Kamber, B.; Riniker, B.; Sieber, P. *Experientia* **1976**, *32*, 246−248.
(10) Segre, G. V.; Rosenblatt, M.; Reiner, B. L.; Mahaffey, J. E.; Potts, J. T., Jr. *J. Biol. Chem.* **1979**, *254*, 6980−6986.
(11) Maton, P. N.; Pradhan, T. K.; Zhou, Z. C.; Gardner, J. D.; Jensen, R. T. *Peptides* **1990**, *11*, 485−489.
(12) Unson, C. G.; Gurzenda, E. M.; Iwasa, K.; Merrifield, R. B. *J. Biol. Chem.* **1989**, *264*, 789−794.
(13) Smith, D. D.; Li, J. H.; Wang, Q.; Murphy, R. F.; Adrian, T. E.; Elias, Y.; Bockman, C. S.; Abel, P. W. *J. Med. Chem.* **1993**, *36*, 2536−2541.
(14) Hoare, S. R. *Drug Discovery Today* **2005**, *10*, 417−427.
(15) Mesleh, M. F.; Shirley, W. A.; Heise, C. E.; Ling, N.; Maki, R. A.; Laura, R. P. *J. Biol. Chem.* **2006**, *282*, 6338−6346.
(16) Nielsen, S. M.; Nielsen, L. Z.; Hjorth, S. A.; Perrin, M. H.; Vale, W. W. *Proc. Natl. Acad. Sci. U.S.A.* **2000**, *97*, 10277−10281.
(17) Rivier, J.; Rivier, C.; Vale, W. *Science* **1984**, *224*, 889−891.

10.1021/ja0760933 CCC: $37.00

Table 1. Analogues of CRF and hUcns and Their Binding Affinities (Inhibitory Binding Constant, K_i (nM)) for Various Receptors[a]

Analog	Name	Sequence	CRF-R1α	CRF-R2β	ECD1-CRF-R1	ECD1- CRF-R2β
1	hCRF	SEEPPISLDLTFHLLREVLEMARAEQLAQ QAHSNRKLMEII-NH_2	1.0 (0.2-4.6)[23]	6.2 (2.0-19)[23]	N.B.[65]	97 (22-430)[65]
2	Astressin	fHLLREVLEXARAEQLAQ EAHKNRKLLEXI-NH_2	2.0 (1.8-2.3)[39]	0.62 (0.49-0.78)[65]	27 (18-41)	10.7 (5.4-21.1)[65]
3	Astressin B	Ac-DLTfHLLREVLEXARAEQZAQ EAHKNRKLXEZI-NH_2	0.56 (0.44-0.74)	1.4 (1.2-1.6)	13 (8.8-20)	3.6 (1.3-9.7)
4	Sauvagine	pEGPPISIDLSLELLRKMIEIEKQEKEKQ QAANNRLLLDTI-NH_2	0.6 (0.3-1.4)	1.6 (0.7-3.8)[65]	N.B.	>200[65]
5	Astressin$_2$-B	Ac-DLSfHZLRKXIEIEKQEKEKQ QAENNKLLLDZI-NH_2	>500	1.3 (0.95-1.7)	N.B.	>300
6	Stressin$_1$	Ac-PPISLDLTfHLLREVLEXARAEQIAQ QEHSKRKLXEII-NH_2	1.7 (1.1-2.6)[23]	222 (137-361)[23]	N.B.	N.B.
7	hUcn1	DNPSLSIDLTFHLLRTLLELARTQSQRE RAEQNRIIFDSV-NH_2	0.4 (0.2-0.8)	0.5 (0.2-1.5)	150 (96-230)	6.5 (6.0-6.9)
8	hUcn2	IVLSLDVPIGLLQILLEQARARAAARE QATTNARILARV-NH_2	> 100[19]	0.50[19] (0.22-1.16)	N.B.	73 (44-120)
9	hUcn3	FTLSLDVPTNIMNLLFNIAKAKNLRA QAAANAHLMAQI-NH_2	>100[19]	14[19] (9.2-19.7)	N.B.	>300

[a] X = norleucine; Z = Cα-methyl-leucine; N.B. = no significant displacement of bound ^{125}I-sauvagine at 1 μM ligand; pE = pyroglutamic acid; f = DPhe. Side chains of residues connected by lines are involved in a lactam bridge.

To understand the mechanism of receptor activation and the structural basis for selectivity of CRF-like ligands and gain insight into the various modes of action, we determined the conformations of the three human urocortins (hUcns) 1,[3] 2,[18] and 3[19] (numbered **7**, **8**, and **9**, respectively, in Table 1) and the three analogues astressin B (**3**),[20,21] astressin$_2$-B (**5**),[22] and stressin$_1$ (**6**)[23] using NMR techniques in dimethylsulfoxide (DMSO)-d_6. DMSO is used as the solvent in the current studies, because in water, CRF has been shown to be either partially structured[24] or unstructured.[1] In addition, the NMR structure of a urocortin 1-based analogue in water,[25] which is presumed to be the bioactive conformation, is very similar to the conformation reported here in DMSO. Astressin B is a nonselective antagonist based on hCRF (**1**) and astressin (**2**); astressin$_2$-B (**5**) is a CRF-R2-selective antagonist based on sauvagine (**4**); and stressin$_1$ (**6**) is a CRF-R1-selective agonist based on hCRF (**1**). Astressin B and hUcn1 bind to CRF-R1 and CRF-R2 with low nanomolar (nM) affinities, stressin$_1$ binds selectively to CRF-R1, while astressin$_2$-B, and hUcn2 and hUcn3 bind selectively to CRF-R2. All of the ligands have amidated C-termini; the three analogues have lactam bridges at different positions in the C terminus (Table 1) and are acetylated at the N terminus.

2. Results

2.1. Chemical Shift Assignment of Protons. Almost complete chemical shift assignments of all of the protons for the six ligands have been identified and are given in Table 2 (complete list of the assignment is given in Supporting Information, Table S1**)**. Since the N terminus is acetylated for analogues **3**, **5**, and **6**, the amide resonances of the first residue were observed in the spectrum including the acetyl group at the N terminus. For ligands **7**−**9**, the HN resonances of the first residue were not observed in the NMR spectrum because they undergo fast exchange with the solvent. The spin systems were identified through the analysis of double quantum filtered correlation spectroscopy (DQF-COSY)[26] and total correlation spectroscopy (TOCSY)[27,28] spectra, and sequential connectivities were identified from the nuclear Overhauser enhancement spectroscopy (NOESY)[29,30] spectrum. Local secondary structure elements can be predicted from the observed αH proton chemical shifts. A plot of the observed chemical shift difference of the αH protons with the corresponding random coil values is shown in Figure 1 except for the unnatural amino acids, such as DPhe, norleucine (Nle), and Cα-methyl-leucine (Cml) whose random coil chemical shift values are not known. Continuous upfield-shifted values (minimum 3−4 residues) are indicative for a preference of a

(18) Reyes, T. M.; Lewis, K.; Perrin, M. H.; Kunitake, K. S.; Vaughan, J.; Arias, C. A.; Hogenesch, J. B.; Gulyas, J.; Rivier, J.; Vale, W. W.; Sawchenko, P. E. *Proc. Natl. Acad. Sci. U.S.A.* **2001**, *98*, 2843−2848.
(19) Lewis, K.; Li, C.; Perrin, M. H.; Blount, A.; Kunitake, K.; Donaldson, C.; Vaughan, J.; Reyes, T. M.; Gulyas, J.; Fischer, W.; Bilezikjian, L.; Rivier, J.; Sawchenko, P. E.; Vale, W. W. *Proc. Natl. Acad. Sci. U.S.A.* **2001**, *98*, 7570−7575.
(20) Rivier, J. E.; Kirby, D. A.; Lahrichi, S. L.; Corrigan, A.; Vale, W. W.; Rivier, C. L. *J. Med. Chem.* **1999**, *42*, 3175−3182.
(21) Rivier, J.; Gulyas, J.; Corrigan, A.; Craig, A. G.; Martinez, V.; Taché, Y.; Vale, W.; Rivier, C. *J. Med. Chem.* **1998**, *41*, 5012−5019.
(22) Rivier, J.; Gulyas, J.; Kirby, D.; Low, W.; Perrin, M. H.; Kunitake, K.; DiGruccio, M.; Vaughan, J.; Reubi, J. C.; Waser, B.; Koerber, S. C.; Martínez, V.; Wang, L. X.; Taché, Y.; Vale, W. *J. Med. Chem.* **2002**, *45*, 4737−4747.
(23) Rivier, J.; Gulyas, J.; Kunitake, K.; DiGruccio, M.; Cantle, J. P.; Perrin, M. H.; Donaldson, C.; Vaughan, J.; Million, M.; Gourcerol, G.; Adelson, D. W.; Rivier, C.; Taché, Y.; Vale, W. *J. Med. Chem.* **2007**, *50*, 1668−1674.
(24) Dathe, M.; Fabian, H.; Gast, K.; Zirwer, D.; Winter, R.; Beyermann, M.; Schumann, M.; Bienert, M. *Int. J. Pept. Protein Res.* **1996**, *47*, 383−393.
(25) Beyermann, M.; Rothemund, S.; Heinrich, N.; Fechner, K.; Furkert, J.; Dathe, M.; Winter, R.; Krause, E.; Bienert, M. *J. Biol. Chem.* **2000**, *275*, 5702−5709.
(26) Rance, M.; Sorensen, O. W.; Bodenhausen, B.; Wagner, G.; Ernst, R. R.; Wüthrich, K. *Biochem. Biophys. Res. Commun.* **1983**, *117*, 479−485.
(27) Davis, D. G.; Bax, A. *J. Am. Chem. Soc.* **1985**, *107*, 2820−2821.
(28) Braunschweiler, L.; Ernst, R. R. *J. Magn. Reson.* **1983**, *53*, 521−528.
(29) Kumar, A.; Ernst, R. R.; Wüthrich, K. *Biochem. Biophys. Res. Commun.* **1980**, *64*, 2229−2246.
(30) Kumar, A.; Wagner, G.; Ernst, R. R.; Wüthrich, K. *J. Am. Chem. Soc.* **1981**, *103*, 3654−3658.

Table 2. Chemical Shift Assignments of Various Protons in DMSO-d_6 for Analogues **3**, **5**−**9**[a]

	astressin B		astressin$_2$-B		stressin$_1$		hUcn1		hUcn2		hUcn3	
residues	NH	αH	NH	αH	NH	αH	NH	αH	NH	αH	NH	αH
CH_3CO	1.82		1.81		1.82							
D2								4.02				
N3							8.81	4.84				
P/I/F4						4.70		4.31	8.03	3.72		4.17
P/S/V/T5						4.36	7.93	4.17	8.35	4.20	8.58	4.30
I/L6					7.82	4.13	7.60	4.28	8.24	4.36	8.00	4.40
S7					7.86	4.27	7.85	4.27	7.84	4.27	8.02	4.29
L/I8					7.97	4.26	7.75	4.10	7.93	4.28	7.92	4.28
D9	8.31	4.48	8.35	4.46	8.17	4.49	8.20	4.52	8.23	4.54	8.21	4.53
L/V10	8.03	4.31	7.98	4.33	7.75	4.29	7.96	4.27	7.67	4.29	7.57	4.29
T/S/P11	7.72	3.96	8.06	4.09	7.68	3.99	7.76	4.06		4.44		4.45
f/F/I/T12	8.48	4.25	8.53	4.08	8.27	4.37	8.02	4.38	8.29	3.89	7.99	4.07
H/G/N13	8.34	4.34	8.06	4.22	8.38	4.51	8.22	4.41	8.47	3.85, 3.75	8.11	4.57
L/Z/I14	8.03	4.19	8.05		8.01	4.22	8.04	4.25	7.75	4.09	7.99	3.95
L/M15	8.08	4.09	8.09	3.94	8.12	4.10	7.93	4.17	7.92	3.95	8.12	4.16
R/Q/N16	8.13	3.97	8.06	3.84	7.97	4.16	8.03	4.13	8.02	3.89	8.01	4.43
E/K/T/I/L17	8.05	4.07	7.95	3.91	8.00	4.17	7.74	4.14	7.65	3.75	7.87	4.15
V/X/L18	7.94	3.74	7.96	3.83	7.95	4.00	8.04	4.19	8.13	4.01	8.03	4.00
L/I/F19	8.06	4.08	8.16	3.69	8.07	4.16	8.22	4.18	8.03	4.10	8.00	4.21
E/N20	8.14	3.96	7.95	4.02	7.90	4.17	8.20	4.16	8.00	3.93	8.17	4.45
X/I/L/Q21	8.09	3.91	8.15	3.75	7.91	4.11	7.87	4.18	8.25	3.91	8.12	3.77
A/E22	8.32	4.05	8.19	3.94	8.07	4.23	8.05	4.19	8.18	4.03	8.06	3.96
R/K23	8.10	4.01	8.22	3.85	7.99	4.17	8.03	4.18	8.02	3.93	8.12	4.16
A/Q/T24	7.83	3.97	8.03	3.92	8.13	4.19	8.02	4.14	7.96	4.02	7.87	4.01
E/Q/R/K25	8.17	3.95	8.15	3.92	8.06	4.13	8.03	4.22	7.91	3.97	8.00	3.93
Q/K/S/A/N26	8.06	3.84	7.91	4.02	7.89	4.17	8.01	4.22	7.88	4.07	8.07	4.41
Z/E/I/Q/A/L27	8.16		8.23	3.93	8.13	4.25	8.03	4.23	7.91	4.10	8.12	4.06
A/K/R28	7.98	3.81	7.81	3.99	7.97	4.11	8.01	4.15	7.72	4.10	8.00	4.00
Q/E/A29	8.16	4.00	7.90	4.02	7.90	4.14	7.91	4.13	7.77	4.15	7.91	4.07
E/Q/R30	8.27	3.99	7.99	4.07	7.97	4.16	8.02	4.24	7.89	4.14	7.97	3.95
A/E31	8.21	4.10	7.99	4.18	8.00	4.20	8.00	4.23	7.98	4.33	7.98	4.05
H/E/T/A32	7.68	4.31	7.81	4.15	8.44	4.52	7.95	4.19	7.80	4.22	7.91	4.10
K/N/S/Q/T/A33	7.76	3.91	8.20	4.47	8.03	4.24	7.89	4.19	7.67	4.16	7.90	4.11
N/K34	8.43	4.37	8.02	4.40	8.20	4.33	8.16	4.53	8.08	4.52	8.05	4.44
R/K/A35	7.91	3.97	7.90	4.09	7.96	4.23	7.92	4.25	7.99	4.15	7.95	4.16
K/L/I/R/H36	7.84	4.10	7.71	4.18	8.01	4.24	7.85	4.08	8.06	4.18	7.70	4.35
L/I37	7.58	3.98	7.68	4.19	8.17	4.01	7.76	4.09	7.61	4.09	8.07	4.17
X/L/F/M38	7.68	4.00	7.62	4.20	8.38	4.25	7.93	4.54	7.95	4.23	7.95	4.23
E/D/A39	7.71	4.01	8.09	4.45	7.95	4.28	8.33	4.56	7.86	4.21	7.83	4.17
Z/I/S/R/Q40	7.50		7.62		7.86	4.19	7.75	4.33	7.95	4.26	7.90	4.16
I/V41	7.25	3.97	7.34	4.02	7.79	4.10	7.66	4.09	7.54	4.10	7.48	4.08
NH_2	7.09, 6.97		7.14, 6.98		7.09, 6.97		7.30, 7.10		7.36, 7.06		7.27, 7.03	

[a] X = norleucine; Z = Cα-methyl leucine.

helical conformation in all analogues.[31] Indeed, the NOEs shown in Figures 2 and 4 are characteristic of a helical conformation. Strong sequential NH−NH NOEs, medium-range αH−NH NOEs, along with αH^i-NH^{i+3}, αH^i-NH^{i+4}, and $\alpha H^i-\beta H^{i+3}$ NOEs observed for all of the ligands provide strong evidence for the conformational preference toward α-helices.[32]

2.2. Structure Determination. The NMR structures of all of the ligands were calculated using the distance and dihedral angle constraints derived from the observed NOEs. The large number of restraints collected from the NOESY spectrum was crucial in defining the quality of the structures (Table 3) and experimental details, and structure calculation procedures are given in the Experimental Section.

2.2.1. Three-Dimensional Structure of Astressin B (3). Astressin B is a modified fragment (9−41) of human CRF; it binds to both CRF-R1 and CRF-R2 with high affinity (Table 1). Its sequence differs from that of human CRF at residues DPhe,[12] Nle,[21,38] Cml[27,40] and with the presence of a lactam bridge connecting the side chains of Glu[30] and Lys[33] similar to astressin with N-terminal acetylation. The introduction of two Cml residues, acetylation of the N terminus, and extension of the N-terminal by three residues conferred longer duration of action as compared with astressin.[20] Continuous negative chemical shift values observed for the αH protons shown in Figure 1A indicate that there is a helical conformation preferred over the entire length of the peptide. The presence of strong sequential NH−NH NOEs, medium-range αH−NH NOEs, along with several αH^i-NH^{i+3}, αH^i-NH^{i+4}, and $\alpha H^i-\beta H^{i+3}$

(31) Wishart, D. S.; Sykes, B. D.; Richards, F. M. *Biochemistry* **1992**, *31*, 1647−1651.
(32) Wüthrich, K. In *NMR of Proteins and Nucleic Acids*; J. Wiley & Sons: New York, 1986.
(33) Rothemund, S.; Krause, E.; Beyermann, M.; Bienert, M. *J. Pept. Res.* **1997**, *50*, 184−192.
(34) Rijkers, D. T.; Kruijtzer, J. A.; van Oostenbrugge, M.; Ronken, E.; den Hartog, J. A.; Liskamp, R. M. *ChemBioChem* **2004**, *5*, 340−348.
(35) Yamada, Y.; Mizutani, K.; Mizusawa, Y.; Hantani, Y.; Tanaka, M.; Tanaka, Y.; Tomimoto, M.; Sugawara, M.; Imai, N.; Yamada, H.; Okajima, N.; Haruta, J. *J. Med. Chem.* **2004**, *47*, 1075−1078.
(36) Kornreich, W. D.; Galyean, R.; Hernandez, J.-F.; Craig, A. G.; Donaldson, C. J.; Yamamoto, G.; Rivier, C.; Vale, W. W.; Rivier, J. E. *J. Med. Chem.* **1992**, *35*, 1870−1876.
(37) Rivier, J.; Rivier, C.; Galyean, R.; Miranda, A.; Miller, C.; Craig, A. G.; Yamamoto, G.; Brown, M.; Vale, W. *J. Med. Chem.* **1993**, *36*, 2851−2859.
(38) Rivier, J.; Lahrichi, S. L.; Gulyas, J.; Erchegyi, J.; Koerber, S. C.; Craig, A. G.; Corrigan, A.; Rivier, C.; Vale, W. *J. Med. Chem.* **1998**, *41*, 2614−2620.
(39) Gulyas, J.; Rivier, C.; Perrin, M.; Koerber, S. C.; Sutton, S.; Corrigan, A.; Lahrichi, S. L.; Craig, A. G.; Vale, W. W.; Rivier, J. *Proc. Natl. Acad. Sci. U.S.A.* **1995**, *92*, 10575−10579.
(40) Beyermann, M.; Fechner, K.; Furkert, J.; Krause, E.; Bienert, M. *J. Med. Chem.* **1996**, *39*, 3324−3330.

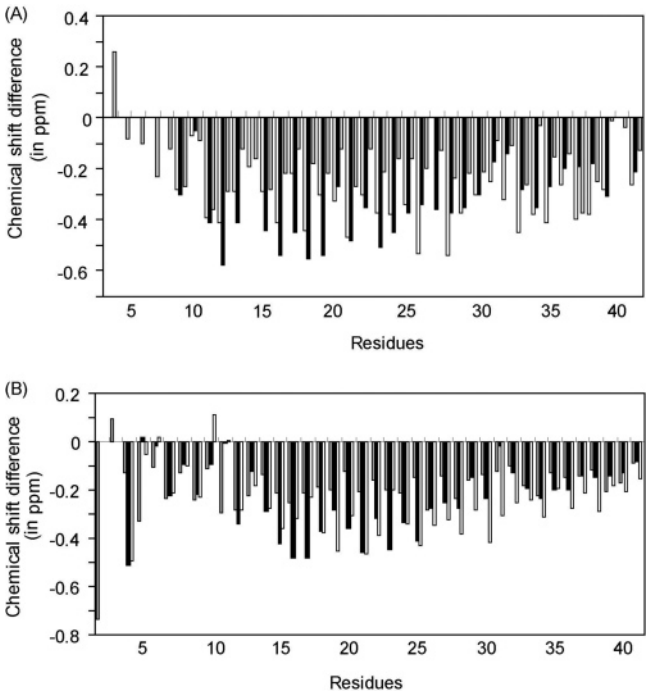

Figure 1. Plot of chemical shift differences of αH protons between observed and random coil values versus residue number of (A) astressin B in white, astressin$_2$-B in black, stressin$_1$ in gray bars and in (B) hUcn1 in gray, hUcn2 in black, hUcn3 in white bars. Continuous negative values suggest a helical conformation in the peptide fragment.

NOEs provides evidence for the conformational preference toward α-helix for residues 11−40. Some of the sequential NOEs could not be observed in the spectrum because of overlapping amide or αH resonances. The presence of $\alpha H^{i}-NH^{i+2}$ NOEs in the C terminus suggests a conformational equilibrium between 3_{10}-helix and α-helix.

In the NMR structure of astressin B, two α-helical segments are observed from residues DPhe^{12} to Gln^{26} and Cml^{27} to Ile,[41] which are at an angle 90° with respect to each other (Figure 3). Both the N- and C-terminal helices are amphipathic in nature. The continuous $CO^{i}-HN^{i+4}$ hydrogen bonds observed in all of the 20 conformers calculated indicate that the helices are stable. The turn motif around Cml^{27} is stabilized by the hydrogen bond between the backbone carbonyl of Glu^{25} and the amide proton of Cml^{27}. The close proximity of the side chains of Glu^{20} with Arg^{16} and Arg^{23}, Lys^{36}, and Glu^{39} suggest that they could be involved in intramolecular salt bridge interactions (Figures 5 and 6).

2.2.2. Three-Dimensional Structure of Astressin$_2$-B (5). Astressin$_2$-B is an antagonist analogue based on sauvagine (11−41), and it binds selectively to CRF-R2 with high affinity (Table 1) although sauvagine binds to both the receptors nonspecifically. It is similar in length to astressin B (one residue shorter) and differs from it at eight positions. In particular, the lactam bridge is between residues 32 and 35 and not between 30 and 33 as in astressin B or astressin. The other unnatural amino acids of astressin$_2$-B are Cml[14,40] and Nle[18] that are suggested to extend its duration of action.[22] Continuous negative chemical shift values observed for the αH protons (Figure 1A) indicate a helical conformation. Comparison of the observed chemical shifts with astressin B suggests that the N terminus (residues 12−25) is more helical in astressin$_2$-B, while the C terminus (residues 26−41) is more helical in astressin B. NOEs characteristic of helices are observed over the entire length of astressin$_2$-B from residues 12 to 41 (Figure 2). Some of the sequential NOEs could not be observed in the spectrum because of degeneracy in the amide proton or αH proton resonances.

The NMR structure of astressin$_2$-B identified two helical segments, from Asp^{9} to Glu^{25} with a kink around residue 28 and from Gln^{29} to Ile^{41} (Figures 3 and 6). The two helical segments are almost perpendicular to one another. The C-terminal helix is mostly hydrophobic, and the N-terminal helix is amphipathic (Figure 6). From the close proximity of the side chains observed in the structure, several intramolecular salt bridges can be formed including Arg^{16} to Glu^{20}, Glu^{22} to Lys^{26}, and Lys^{23} to Glu^{27} (Figure 6).

2.2.3. Three-Dimensional Structure of Stressin$_1$ (6). Stressin$_1$ is an agonist analogue of human CRF that binds selectively to CRF-R1 with high nanomolar affinity (Table 1).[23] It differs from human CRF in that three residues in the N terminus are deleted, the N terminus is acetylated, it has the unnatural amino acids DPhe^{12} and Nle,[21,38] and the lactam bridge is between Glu^{31} to Lys.[34] The position of the lactam bridge differs from the position in both astressin B and astressin$_2$-B. The chemical shift difference plot for the αH protons of stressin$_1$, shown in Figure 1A, suggests that a helical conformation is preferred from residues 6 to 38 and that the C terminus is unstructured. The chemical shift values observed indicate that the overall helical content is less, compared to that of astressin B and astressin$_2$-B. Furthermore, NOEs indicative of a helical conformation are observed only from Asp^{9} to Arg^{35} (Figure 2).

The NMR structure of stressin$_1$ shows that residues 12−35 prefer an α-helical conformation, while residues 4−11 at the N terminus and 36−41 at the C terminus remain unstructured (Figure 3). This structure is very similar to the conformation of human or ovine CRF reported in a water/TFE mixture.[33] Residues Arg^{16} and Glu^{20} are in close proximity, favoring a salt bridge interaction (Figure 7). Although the structure is a long helix, there is a small kink observed at Ile^{27}, very similar to that reported for astressin in DMSO.[1]

2.2.4. Three-Dimensional Structure of hUcn1 (7). Human Ucn1 binds to both the CRF receptors with high nanomolar affinity (Table 1). It differs from hCRF at 15 positions, nine of which are in the region 25−33. The chemical shift difference plot of the αH protons (Figure 1B) suggests that residues 4−41 have a preference for a helical conformation. Helical NOEs characteristic of α-helix are observed from residues 5−38 (Figure 4) and could not be observed after Ile^{37} because of the degeneracy in the HN and αH chemical shifts (Table 2).

The NMR structure of hUcn1 is helical with two α-helical segments (Figure 3) from Thr^{11} to Leu^{18} and Leu^{21} to Ile^{37}, respectively. The C-terminal residues Phe^{38} to Val^{41} do not have a well-defined structure among the 20 conformations calculated; some of them have a preference for 3_{10}-helix over α-helix. Both the N- and C-terminal helices are amphipathic in nature, and the C-terminal helix has a small curvature (Figure 7).

2.2.5. Three-Dimensional Structure of hUcn2 (8). Human Ucn2 binds selectively to CRF-R2 with high affinity (Table 1) and is more cationic and shorter in length than hUcn1 by two residues at the N terminus. The chemical shift difference plot

(41) Barazza, A.; Wittelsberger, A.; Fiori, N.; Schievano, E.; Mammi, S.; Toniolo, C.; Alexander, J. M.; Rosenblatt, M.; Peggion, E.; Chorev, M. *J. Pept. Res.* **2005**, *65*, 23−35.

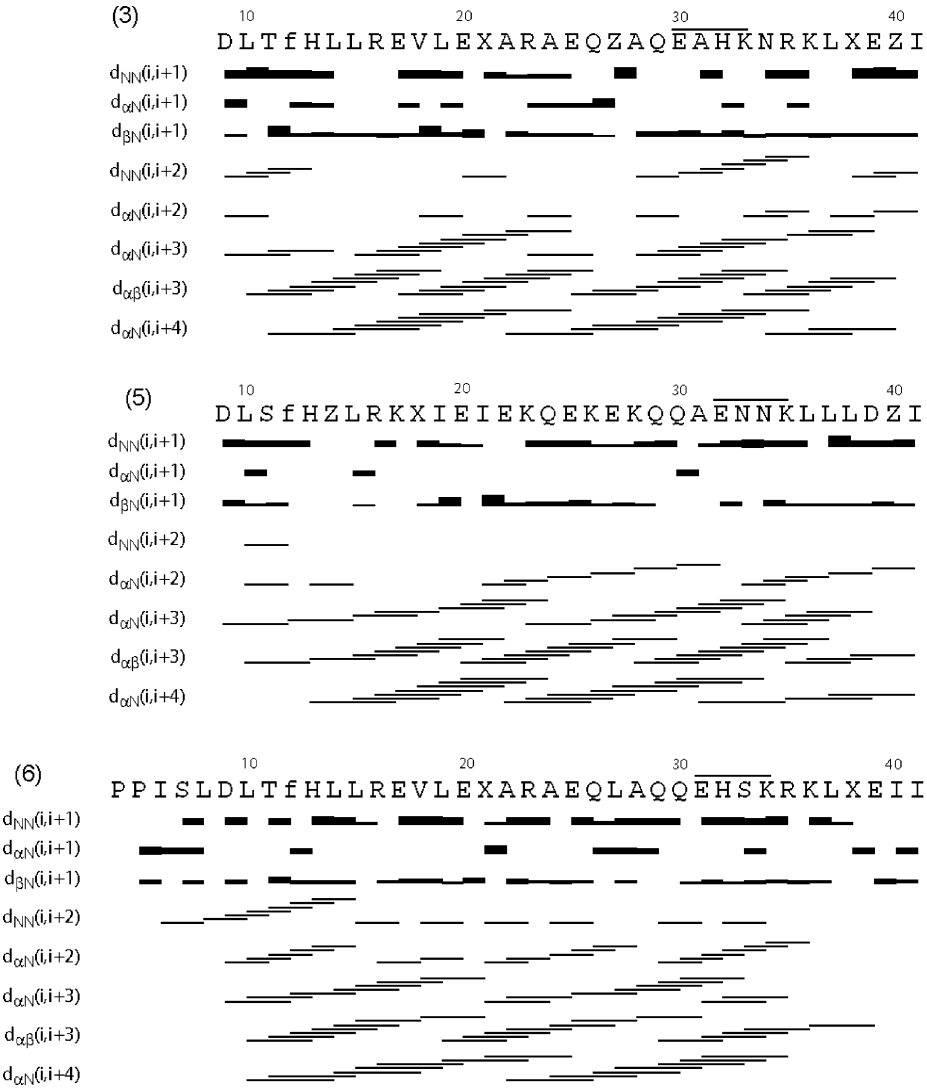

Figure 2. Survey of characteristic NOEs used in CYANA for structure calculation for (**3**) astressin B, (**5**) astressin$_2$-B and (**6**) atressin$_1$. Light gray, thin, medium, and thick bars represent very weak (4.5−6 Å), weak (4−4.5 Å), medium (3−4 Å), and strong (<3 Å) NOEs observed in the NOESY spectrum. The medium-range sequential connectivities $d_{NN}(i,i+2)$, $d_{\alpha N}(i,i+2)$, and $d_{\beta N}(i,i+2)$ are shown by lines starting and ending at the positions of the residues related by the NOE. Residues designated with f, X, and Z correspond to the amino acids DPhe, Nle (norleucine), and Cml (Cα-methylleucine), respectively. The bar indicates the presence of the lactam bridge connecting the side chains of the residues Glu^{30} and Lys^{33}.

for the αH protons (Figure 1B) suggests that residues 12−41 have a preference for a helical conformation. Observed chemical shift dispersion for the αH protons indicates that the helical content is more pronounced in hUcn2 than in hUcn1, especially in the N-terminal residues 14−30. Several $\alpha H^{i}-NH^{i+3}$, $\alpha H^{i}-NH^{i+4}$, and $\alpha H^{i}-\beta H^{i+3}$ NOEs characteristic of α-helix are observed from Ile^{12} to Arg^{40} (Figure 4).

The NMR structure shows two α-helical regions from residues Ile^{12} to Ala^{22} and Arg^{23} to Ala^{39}, respectively (Figure 6), that are oriented at 90° with respect to each other (Figure 3). Residues 4−11 at the N terminus remain unstructured, similar to the structures of stressin$_1$ and hUcn1. The three-dimensional (3D) structure shows that the C-terminal helix is amphipathic (Figure 5), and all of the residues in the N-terminal helix are hydrophobic except Asp^{9} and Glu^{20} (Figure 6). The last three residues at the C terminus of hUcn2 are in an extended conformation. Human Ucn2 is the only ligand with Ala at position 39, while all of the other analogues have Asp or Glu, whose side chain is proposed to be involved in a salt bridge with Lys or Arg at position 36.[1]

2.2.6. Three-Dimensional Structure of hUcn3 (9). Human Ucn3 also binds selectively to CRF-R2 with high affinity (Table 1) but is relatively less potent compared to hUcn2. It is similar in length to hUcn2 and is more cationic than hUcn1 and hUcn2. The chemical shift difference plot for the αH protons shown in Figure 1B suggests that residues 12−41 have a preference for a helical conformation. Although the chemical shift dispersion observed for the αH protons is very similar to that in hUcn2, there are fewer NOEs characteristic of an α-helix (in particular in the C-terminal region of the ligand after Ala^{35}, Figure 4).

The NMR structure of hUcn3 comprises a single helical fragment from residues Thr^{12} to Asn^{34} with extended N- and C-terminals (Figures 3 and 7).

3. Discussion

The NMR structures of six chemically divergent CRF analogues have been determined in DMSO (Figures 6 and 7). A detailed comparison of these 3D structures along with binding studies are discussed here in order to identify residues possibly involved in receptor binding and selectivity. Furthermore, the

Table 3. Structural Statistics of Astressin B, Astressin$_2$-B, Stressin$_1$, hUcn1, hUcn2 and hUcn3

parameters	astressin B	astressin$_2$-B	stressin$_1$[a]	hUcn1[b]	hUcn2[c]	hUcn3[d]
Constraints						
no. of NOE upper distance limits	682	700	536	610	726	468
no. of dihedral angle constraints	81	80	118	138	121	122
residual target function (Å^2)	0.39 ± 0.1	0.11 ± 0.02	0.17 ± 0.06	0.09 ± 0.02	0.20 ± 0.01	0.11 ± 0.04
no. of residual NOE violations >0.2 Å	3.00 ± 0.4	0.60 ± 0.1	1.10 ± 0.4	1.60 ± 0.2	2.60 ± 0.1	1.20 ± 0.3
maximum violation (Å)	3.70 ± 0.4	1.00 ± 0.1	2.00 ± 0.4	2.00 ± 0.2	2.90 ± 0.1	1.70 ± 0.3
angle violation (deg)	0.90 ± 0.3	0.00 ± 0.1	2.40 ± 1.4	0.00 ± 0.0	0.00 ± 0.0	0.00 ± 0.1
Energies (kcal/mol)						
total	−329 ± 113	−288 ± 143	−373 ± 186	−768 ± 48	−468 ± 29	−337 ± 27
van der Waals	−44 ± 15	−41 ± 12	−42 ± 18	−76 ± 15	−22 ± 12	−57 ± 17
electrostatic	−440 ± 71	−329 ± 155	−453 ± 150	−788 ± 54	−534 ± 42	−354 ± 34
Atomic Pairwise RMSD (Å)						
backbone atoms	0.66	0.87	0.98	0.99	0.15	0.29
heavy atoms	1.02	1.36	1.62	1.33	0.58	0.86
Structural Analysis						
residues in disallowed region (%)	0.0	7.6	1.6	0.0	0.0	1.0
residues in gen. allowed region (%)	4.5	6.8	3.5	0.7	2.7	2.0
residues in allowed region (%)	14.5	20.8	28.4	5.9	15.5	22.4
residues in most favored region (%)	81.0	64.8	66.5	93.4	81.9	74.6

[a] Backbone and heavy atom RMSDs reported are obtained by superimposing residues from 13 to 27. [b] Backbone and heavy atom RMSDs reported are obtained by superimposing residues from 9−40. [c] Backbone and heavy atom RMSDs reported are obtained by superimposing residues from 5 to 41. [d] Backbone and heavy atom RMSDs reported are obtained by superimposing residues from 8 to 37.

3D structures might give insight into the plurality of actions of the six CRF-like peptides binding to the two CRF receptors.

3.1. Comparison of the C-Terminal Helices of the CRF Analogues with the Reported Bioactive Conformation of Astressin. In the structure of the ECD1-CRF-R2−astressin complex reported recently by our group, it was observed that most of the residues involved in the ECD1−astressin interactions are of hydrophobic nature.[1] The C-terminal resiudes of astressin from Leu^{27} to Ile^{41} thereby interact with the ECD1 of the CRF receptor as an amphipathic α-helix.[15] Residues of astressin interacting with the ECD1 are Leu^{27}, Ala^{31}, Asn^{34}, Arg^{35}, Leu^{37}, Nle^{38}, Ile^{40}, and Ile^{41}, part of the hydrophobic face (Figure 5A). Residues that are part of the hydrophilic face, namely Gln^{29}, His^{32}, Lys^{33}, Lys^{36}, and Glu^{39}, are solvent exposed. Detailed comparison of the structures of the C-terminal amphipathic helices from 27 to 41 shows that the conformations of the free ligands in DMSO are very similar to the conformation of astressin in complex with the ECD1 of CRF-R2 (Figure 5).[1] This includes, in particular, the hydrophilic face of the helix comprising residues Ala/Arg/Lys^{28}, Gln/Glu^{29}, His/Glu/Thr^{32}, Lys/Ile/Arg/Leu^{36}, and Glu/Asp/Ala^{39}, which are not conserved among the ligands. In addition, the residues of the hydrophobic face involved in receptor binding are conserved or conservatively substituted except for the lactam bridge (see below). The similarity of the conformations of the C-terminal amphipathic helix, which is involved in binding to the receptors, for five of the six ligands studied (Figure 5), indicates that astressin B, astressin$_2$-B, and hUcn1−3 possibly bind to the ECD1 of the receptors in a similar fashion as astressin.[1]

Since the ligands are unstructured or only partially structured in H_2O,[1,24,33] a prerequisite for binding is that the C-terminal residues 30−41 fold into a helical conformation. This correlates well with data reported for the short analogues, acetylated residues 27−41[34] or 30−41[35] which show only high binding affinities when the lactam bridge is introduced. The linear analogues are reported to have no binding to the ECD1, suggesting partial folding is enabled by the lactamization of the side chains of Glu^{30} and Lys^{33}.

3.2. Structure−Activity Relationship by Correlation of Site-Specific Ala Scan Studies of Ovine CRF with the 3D Structures of the Analogues. Single site-directed Ala substitution studies on ovine CRF (oCRF) have been reported which identify the importance of each amino acid side chain for in vitro potency on CRF-R1.[36] These studies show a complete loss of potency when hydrophobic residues at positions 6, 8, 10, 12, 14, and 38 are replaced by alanine (Ala), suggesting that these residues are crucial for receptor binding.[36] Further, Ala replacement at positions 7, 9, 13, 15, 16, 19, and 35 also result in loss of potency over a range of 30−60%. In contrast, Ala replacement for residues 20, 22, 26, 32, 33, 39, and 40[36] enhances potency 2−5 times. Since Ala is a helix inducer and the formation of a helix is important for potency in CRF-like ligands, it is assumed that loss of potency by an Ala replacement is indicative of the involvement of the corresponding amino acid side chain in binding to the receptor. In contrast, an enhancement of potency by an Ala replacement suggests that the corresponding amino acid side chain is not involved in binding. Analyzing the mutagenesis studies under this assumption along with the positioning of these residues in the 3D structures of these ligands suggests that all of the residues 6−16 are involved in receptor binding, whereas for the remaining part of the ligand, only its hydrophobic face is involved in binding (Figures 6 and 7).

3.3. Correlation of Site-Specific D-Residues, Lactam Bridge Scan, and Other Replacement Studies with the 3D Structures of CRF Ligands. Further information about receptor binding can be gained by single D-amino acid replacement, since D-amino acids have been shown to destabilize the structure by introducing a turn or a twist. The D-amino acid scan of oCRF shows that single-point D-amino acid replacement is not tolerated for the first 11 residues and also at positions 13, 16, 31, 34, and 38 for CRF-R1.[37] The importance in receptor binding of the first 11 residues as well as residues 31, 34, and 38 of the hydrophobic face of the C-terminal helix is therefore highlighted again.[1]

Complementary information can be obtained from lactam bridge scans, because such bridges from residue *i* to *i*+3 or

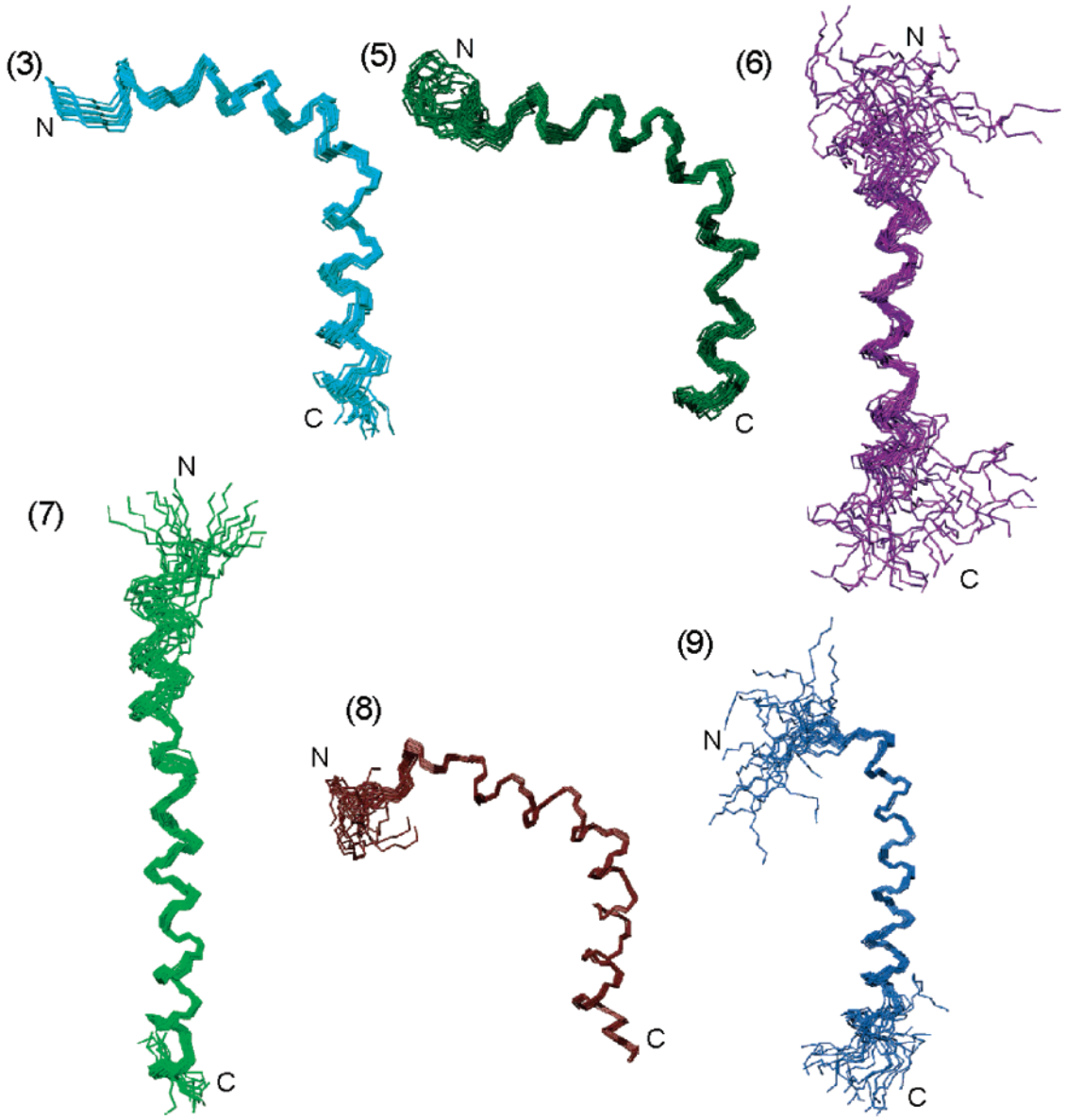

Figure 3. NMR structures of (**3**) astressin B in cyan, (**5**) astressin$_2$-B in dark green, (**6**) stressin$_1$ in purple, (**7**) hUcn1 in green, (**8**) hUcn2 in brown, and (**9**) hUcn3 in royal blue. For each analogue, 20 energy-minimized conformers are shown as a bundle, and the conformers with the lowest target function are used to represent the NMR structure. The bundle is obtained by superposition of C^{α} atoms of the residues 13−41 except for stressin$_1$ and hUcn3. For stressin$_1$ and hUcn3, C^{α} atoms of the residues 16−30 and 13−34, respectively, were superimposed to obtain the bundle. The N- and C-terminals of the analogues are marked for clarity, and only the backbone of the analogues is displayed.

i+4 may induce helical conformations. The lactam bridge scans reported in the literature show that the introduction of a lactam bridge at position 20−23 or 30−33 enhances potency,[36,38] although residues at these positions, namely Glu^{20}, Lys^{23}, and Gln^{30}, are highly conserved among the ligands (except for Ser^{33}). The rationale for the observed potency increase resulting from the introduction of the lactam bridge Glu^{20}-Lys^{23} is that it may mimic a salt bridge interaction between Glu^{20} and Lys^{23} present on the hydrophilic face of the 3D structures determined (Figure 5). This suggests that residues 20−23 are part of a helical active conformation as suggested by the NMR studies. Similarly, the lactam bridge between residues 30−33 induces a helical conformation, which is crucial for binding to the ECD1.[1] This interpretation is further strongly supported by the observation that analogues with a lactam bridge at position 30−33 bind much better when compared to the corresponding linear analogues.[34,35,39] However, since residues 30 and 33 are part of the hydrophobic face of the C-terminal helix of the ligand, lactamization of these side chains may also alter the binding affinities to the receptor in a receptor-specific manner (see below).

Conservative substitutions at positions 5−14 (except 12) result in loss of activity, suggesting that all of these side chains are important in receptor interaction.[40] For example, small changes in the length of the side chains of residues 16, 17, 30, 31, 34, and 35 have a dramatic negative effect on potency. These residues Gln^{30}, Ala^{31}, Asn^{34}, and Arg^{35} are highly conserved in sequence and also in their position in the 3D structures of the ligands. Furthermore, all of these residues are observed to be interacting with the ECD1 in the structure of the astressin−ECD1 complex.[1] In particular, Gln^{30} and Asn^{34} are involved in intermolecular hydrogen bonds for which exact length of the side chains is crucial for hydrogen bond formation. Similarly,

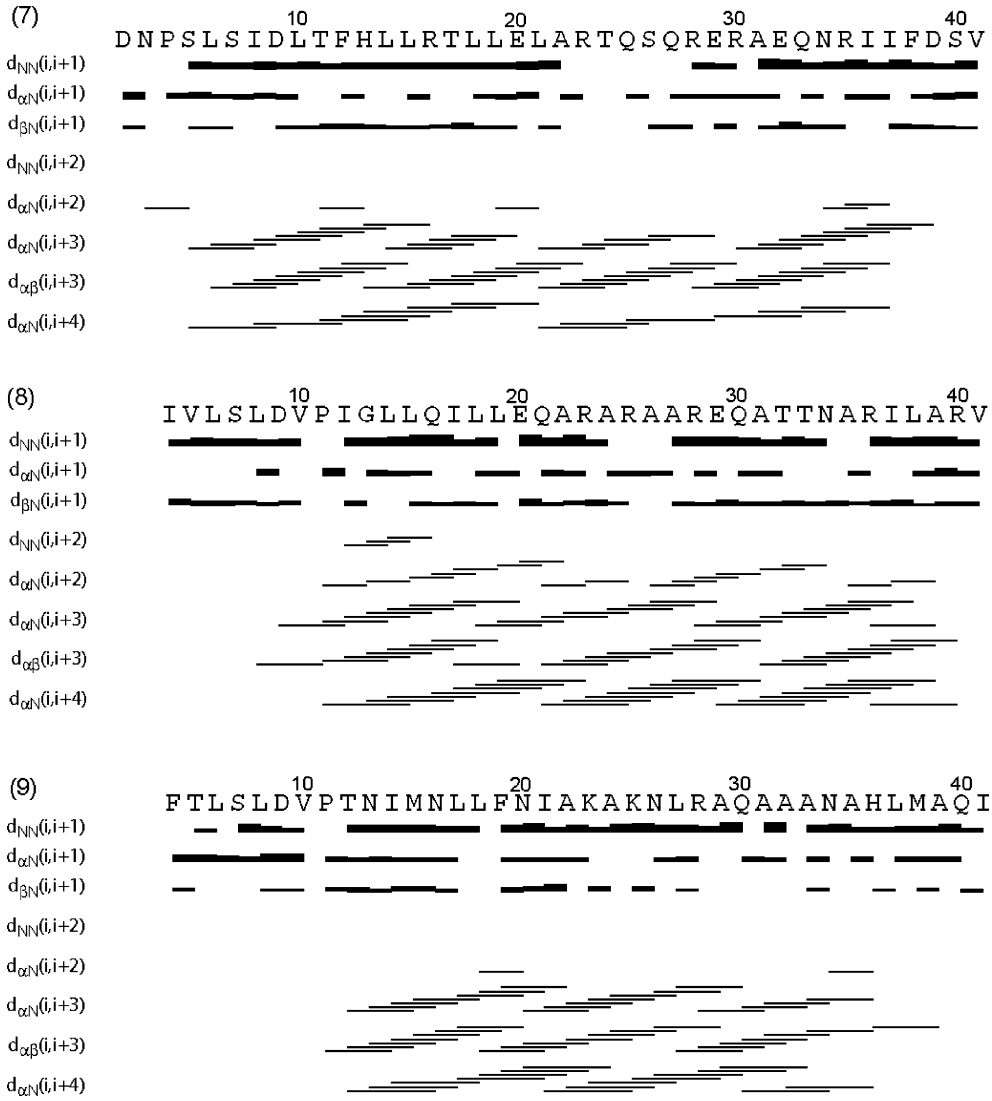

Figure 4. Survey of characteristic NOEs used in CYANA for structure calculation for (**7**) hUcn1, (**8**) hUcn2, and (**9**) hUcn3. Light gray, thin, medium, and thick bars represent very weak (4.5−6 Å), weak (4−4.5 Å), medium (3−4 Å), and strong (<3 Å) NOEs observed in the NOESY spectrum. The medium-range sequential connectivities $d_{NN}(i,i+2)$, $d_{\alpha N}(i,i+2)$, and $d_{\beta N}(i,i+2)$ are shown by lines starting and ending at the positions of the residues related by the NOE.

the highly conserved Ala[31] is involved in a hydrophobic interaction, and there is not sufficient space to accommodate a residue having a longer side chain such as that of Leu.[40] Finally, Lys replacement for Arg[35] is also not tolerated since Arg[35] is involved in an intermolecular salt bridge interaction with the ECD1.[1]

The good correlation between the biological data on conservative residue substitutions and the 3D structures of the ligands suggests that the significant potency loss on substituting Arg[16] by Lys[16] and Glu[17] by Asp[17] may be due to receptor−ligand interaction at these residues. In particular, the loss of potency reported, when Asp replaces Glu[17], suggests that Glu[17] may be involved in an intermolecular salt bridge interaction with the receptor. This conclusion is further supported by the 3D structure, since Glu[17] is part of the hydrophobic face proposed to be interacting with the receptor. An alternative explanation could be proposed for Arg[16], whose side chain is part of the hydrophilic face of the N-terminal helix. Since the side chains of Arg[16] and Glu[20] are in close proximity in the 3D structures of the ligands studied in DMSO, they could be forming an intramolecular salt bridge stabilizing the helix, which is proposed to be the active conformation (Figure 6). Concurrence of the single-point substitution studies and 3D structures suggest that the ligands interact with the receptor along their hydrophobic face from residues 17 to 41 and that residues 1−16 interact over their entire surface with the receptor. Similar conclusions have been reported for PTH ligands.[41]

3.4. Selectivity of CRF Ligands for CRF-R1 and CRF-R2. Among the agonists in the CRF family ligands, CRF, Ucn1, and sauvagine bind nonselectively to both the receptors (CRF-R1 and CRF-R2), whereas oCRF is partially selective to CRF-R1 and Ucn2 and -3 bind selectively to CRF-R2. Similarly, CRF-based antagonists, such as astressin and astressin B (Table 1) bind to both the receptors, while astressin$_2$-B based on sauvagine shows selective binding to CRF-R2 (Table 1). A comparison of the N-terminal sequence of human Ucn2 and -3 with hCRF shows that three amino acids Pro[11]-Ile[12]-Gly[13] in Ucn2 or Pro[11]-Thr[12]-Asn[13] in hUcn3 are different from Thr[11]-Phe[12]-His[13] in hCRF. On the basis of the fact that Pro usually introduces a break in the structure (Figure 6), Jahn et al.

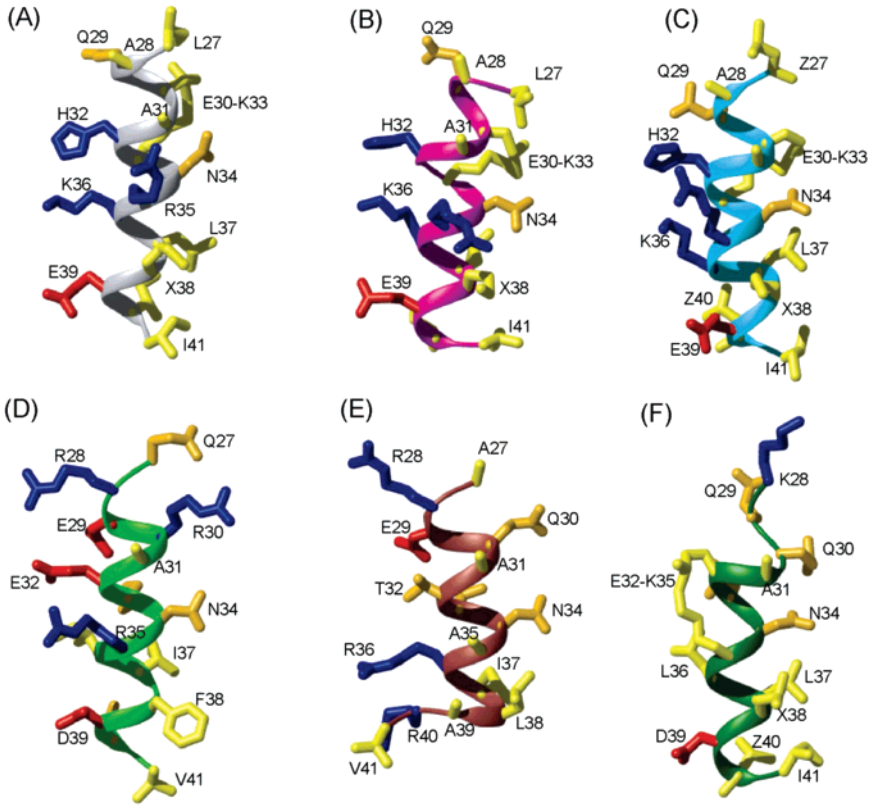

Figure 5. Comparison of the NMR structures of C-terminal helical residues from 27 to 41 of various analogues, (A) astressin bound to ECD1,[1] (B) free astressin, (C) free astressin B, (D) free hUcn1, (E) free hUcn2, and (F) free astressin$_2$-B. The conformer with the lowest target function is displayed. The side chains of hydrophobic residues and the lactam bridges are colored yellow, positive residues in blue, and negative residues in red. Side chains of the residues Thr, Ser, Gln, and Asn are colored orange, and the backbones are displayed as helical ribbons with the following color code: bound astressin in gray, astressin in magenta, astressin B in cyan, hUcn1 in light green, hUcn2 in brown, and astressin$_2$-B in dark green. The side chains of the residues are marked for clarity. Residues marked f, X, and Z refer to DPhe, Nle, and Cml, respectively.

suggested that these residues decrease the α-helicity and hence impair the binding to CRF-R1.[42] By inserting the three-residue fragments in r/hCRF, they have reported that these peptides[42] show a dramatic decrease (3 orders of magnitude) in the binding affinity to CRF-R1. Structurally, this correlates well with the circular dichroism data, which showed a decrease in α-helical content when the Pro^{11}-Ile^{12}-Gly^{13} segment is introduced in hCRF.[42]

Comparison of the 3D structures of hUcn1, -2, and -3 also shows that there is a difference in the N-terminal helices of hUcn2 and -3, which do not have any well-defined structures beyond Pro^{11} when compared to hUcn1 (Figures 6 and 7). The N-terminal helix of hUcn1 is also longer than those of hUcn2 and Ucn3 (Figure 7). Furthermore, this region is an amphipathic helix in hUcn1 with Asp^{9}, His^{13}, Arg^{16}, and Glu^{20} on the hydrophilic face and residues Val^{10}, Thr^{11}, Phe^{12}, Leu^{14}, Leu^{15}, Thr^{17}, Leu^{18}, and Leu^{19} on the hydrophobic face of the helix (Figure 7B). Such an amphipathic helix in the N terminus is also observed for stressin$_1$, binding selectively to CRF-R1. In contrast, in hUcn2 and hUcn3 this region does not have charged residues except for residues Asp^{9} and Glu^{20}. These observations suggest that the amphipathic N-terminal helix could play a significant role in CRF-R1 binding and the selectivity for the receptor. This suggestion, however, does not fit with the finding that, although astressin$_2$-B has an amphipathic N-terminal helix (Figure 6B), it does not bind to CRF-R1 (Table 1). Alternatively, residues 5−8 could also contribute to the selectivity of the receptor, in particular Pro^{5}, which is conserved among the ligands binding to CRF-R1. In addition, CRF-R2 selectivity of anti-sauvagine analogues has been reported, when Leu^{12} (sauvagine) is replaced by Tyr and Glu^{13} (sauvagine) is replaced by His.[43]

A detailed comparison of the C-terminal helices of the various analogues (Figure 5) shows that the varied amino acid side chains in the hydrophobic face of the ligand involved in binding to the receptors are located in two clusters around residues 30−35 and 38−41, respectively.[1] The latter cluster at the C terminus is not considered to be important for receptor selectivity since the nonselective astressin B and the CRF-R2-selective astressin$_2$-B comprise a very similar side chain arrangement at the C terminus. However, the cluster around residues 30−35 appears to be involved in receptor-specific binding.[1] In particular, Arg^{35} could play a role in the selectivity, since hUcn2 and hUcn3 have Ala instead of Arg^{35}, and this residue, part of the hydrophobic face of the C-terminal helix, has been shown to be involved in binding to CRF-R2 (Figure 5). In the structure of the ECD1−astressin complex, Arg^{35} is involved in an intermolecular salt bridge with Glu^{86} of the ECD1 in CRF-R2. In CRF-R1, Glu^{86} is replaced by Ala, and hence it

(42) Jahn, O.; Tezval, H.; van Werven, L.; Eckart, K.; Spiess, J. *Neuropharmacology* **2004**, *47*, 233−242.

(43) Brauns, O.; Brauns, S.; Jenke, M.; Zimmermann, B.; Dautzenberg, F. M. *Peptides* **2002**, *23*, 1817−1827.

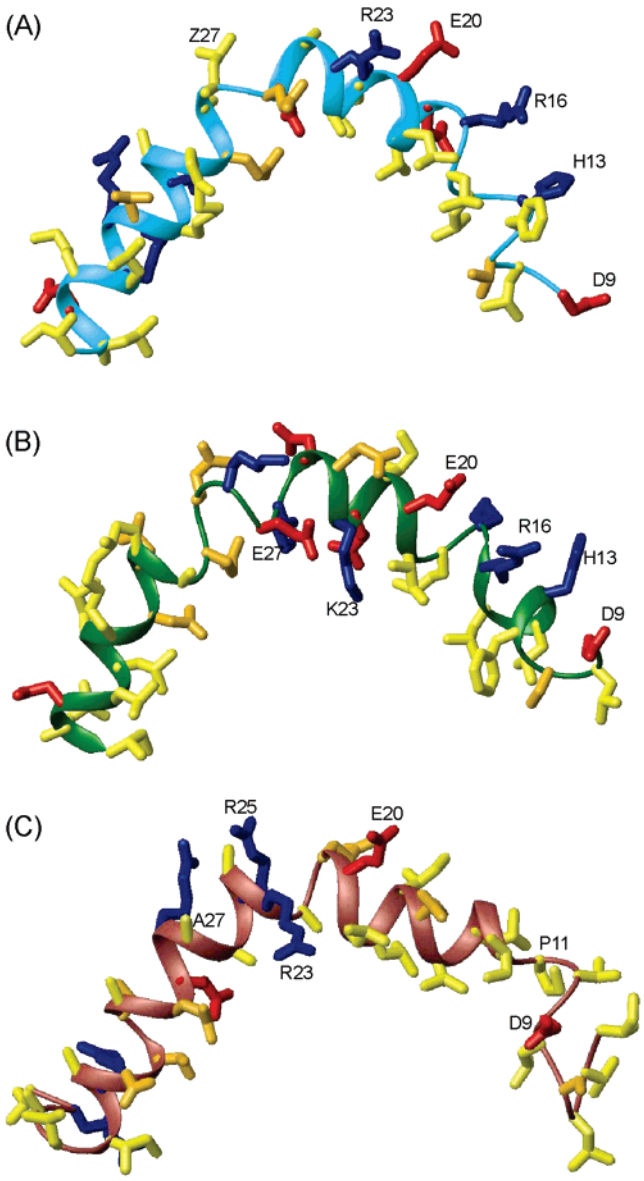

Figure 6. Comparison of the NMR structures of (A) astressin B, (B) astressin$_2$-B, and (C) hUcn2, observed with the large kink between N- and C-terminal helices. The conformer with the lowest target function is displayed. The side chains of hydrophobic residues are colored yellow, positive residues in blue and negative residues in red. Side chains of the residues Thr, Ser, Gln, and Asn are colored orange, and the backbones are displayed as helical ribbons with the following color code: astressin B in cyan, astressin$_2$-B in dark green, and hUcn2 in brown. Residues marked f, X, and Z refer to DPhe, Nle, and Cml, respectively.

has been suggested that in CRF-R1 binding, Arg^{35} could be interacting with Glu^{120}, thus forming a solvent-exposed salt bridge.[1]

3.5. Ligand Binding Model for CRF Family Ligands. The CRF-like peptide hormones activate their receptors by a two-step binding process. Initially, the C-terminal segment of the peptide ligand binds in a helical conformation to the ECD1 of the CRF receptor.[1] Formation of this complex aligns the ligand with respect to the juxtamembrane region of the receptor, enabling receptor activation through interaction between the serpentine segments of the receptor and the N-terminal segment of the ligand.[6−14,16] Further, the relative orientation between the ECD1 and the serpentine regions of the receptor, which are connected by a 15-residue linker, may be determined by the ligand. The 3D structures of the analogues presented here have either a small kink around residues 25−27 for the ligands astressin,[44] stressin$_1$, hUcn1, and hUcn3, or a large kink in astressin B, astressin$_2$-B, and hUcn2. The observed kink orients the N- and C-terminal helices at almost 90°. Therefore, two different orientations between the ECD1 and the transmembrane region of the receptor could be induced by the ligand. In the orientation induced by astressin B, astressin$_2$-B, or hUcn2 comprising a large kink, the ECD1 is oriented along its positively charged face on the membrane, thereby interacting with the extracellular loops 2, 3, and 4 that are mostly negatively charged (Figure 8A). If the ligands have a conformation with a smaller kink as in astressin or hUcn1 or no kink with single long amphipathic helices as in stressin$_1$ or hUcn3, the flexible ECD1 has to be oriented almost 90° compared to its orientation in the previous model so that the N terminus of the ligands can interact with the juxtamembrane region of the receptor (Figure 8B). This suggests a possible peptide hormone-dependent orientation between the ECD1 and the transmembrane region of the receptor, which may alter the peptide hormone-induced signal pathway.

Ligand-dependent structural variations suggested for the ligand−receptor complex may thereby be the basis for the recently proposed differential regulation of receptor-coupled pathways, namely agonist-selective signaling, agonist-selective G-protein selection, and ligand-dependent posttranslational modifications of the receptor as well as its internalization.[45,46] For example, several single amino acid replacements at the N-terminal positions 6−15 of Ucn1 did not affect the binding affinity to CRF-R1, conserved the Gs-protein activity, but were devoid of Gi activity.[45] Another example is that CRF-like peptides, by binding to CRF-R2, initiate a signal through multiple G-proteins[47] or through a G-protein-independent pathway.[48] Thus, the absence or presence of the kink in the ligands, which has been also observed for other B1 peptide hormones,[49−51] might therefore influence the signaling pathway, thereby explaining the complexity and variety of the actions of peptide hormones.

3.6. Correlation of CRF-Mutant Studies for CRF-Binding Protein with the 3D Structures. The clearance of CRF from peripheral plasma, especially during pregnancy, has been associated with the binding of CRF and possibly Ucn1 to the CRF-binding protein (CRF-BP),[52] which is a human plasma

(44) Grace, C. R. R.; Cervini, L.; Gulyas, J.; Rivier, J.; Riek, R. *Biopolymers* **2007**, *87*, 196−205.
(45) Beyermann, M.; Heinrich, N.; Fechner, K.; Furkert, J.; Zhang, W.; Kraetke, O.; Bienert, M.; Berger, H. *Br. J. Pharmacol.* **2007**, *151*, 851−859.
(46) Grammatopoulos, D. K.; Chrousos, G. P. *Trends Endocrinol. Metab.* **2002**, *13*, 436−444.
(47) Teli, T.; Markovic, D.; Levine, M. A.; Hillhouse, E. W.; Grammatopoulos, D. K. *Mol. Endocrinol.* **2005**, *19*, 474−490.
(48) Brar, B. K.; Jonassen, A. K.; Egorina, E. M.; Chen, A.; Negro, A.; Perrin, M.; Mjos, O. D.; Latchman, D. S.; Lee, K.-F.; Vale, W. *Endocrinology* **2004**, *145*, 24−35.
(49) Marx, U. C.; Austermann, S.; Bayer, P.; Adermann, K.; Ejchart, A.; Sticht, H.; Walter, S.; Schmid, F. X.; Jaenicke, R.; Forssmann, W. G.; Rösch, P. *J. Biol. Chem.* **1995**, *270*, 15194−15202.
(50) Marx, U. C.; Adermann, K.; Bayer, P.; Meyer, M.; Forssmann, W. G.; Rosch, P. *J. Biol. Chem.* **1998**, *273*, 4308−4316.
(51) Digilio, G.; Barbero, L.; Bracco, C.; Corpillo, D.; Esposito, P.; Piquet, G.; Traversa, S.; Aime, S. *J. Am. Chem. Soc.* **2003**, *125*, 3458−3470.
(52) Potter, E.; Behan, D. P.; Fischer, W. H.; Linton, E. A.; Lowry, P. J.; Vale, W. W. *Nature* **1991**, *349*, 423−426.

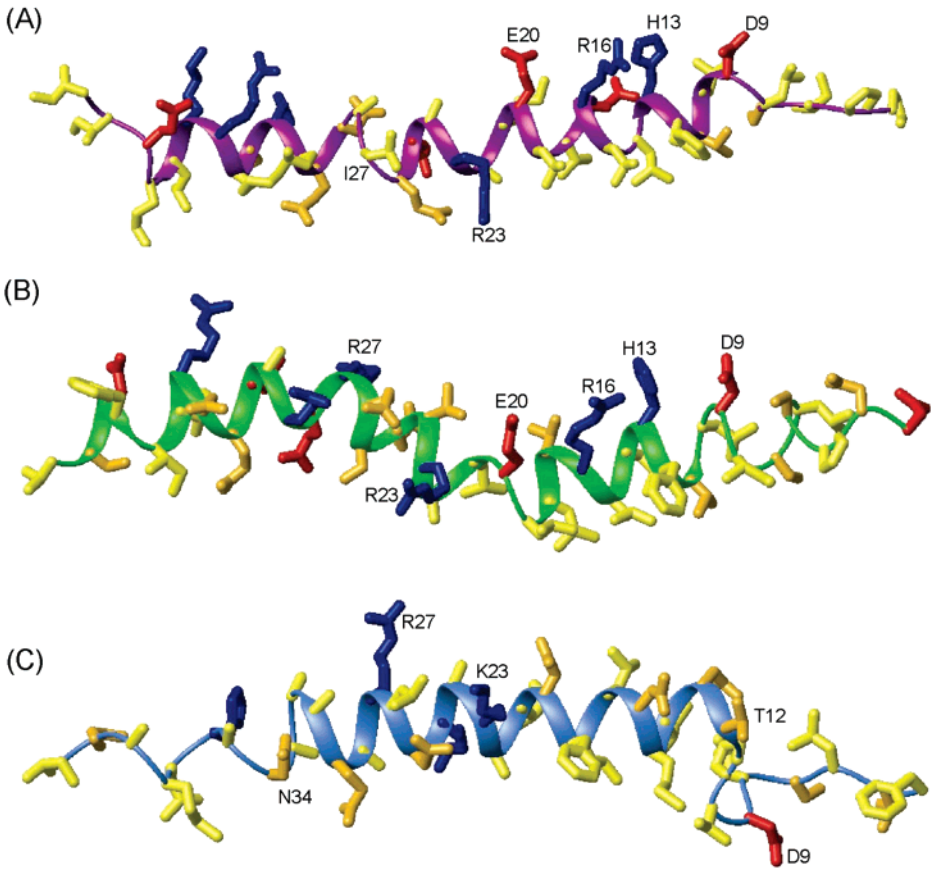

Figure 7. Comparison of the NMR structures of (A) stressin$_1$, (B) hUcn1, and (C) hUcn3, observed with a small or no kink between N- and C-terminal helices. The conformer with the lowest target function is displayed. The side chains of hydrophobic residues are colored yellow, positive residues in blue and negative residues in red. Side chains of the residues Thr, Ser, Gln, and Asn are colored orange, and the backbones are displayed as helical ribbons with the following color code: stressin$_1$ in violet, hUcn1 in green, and hUcn3 in royal blue.

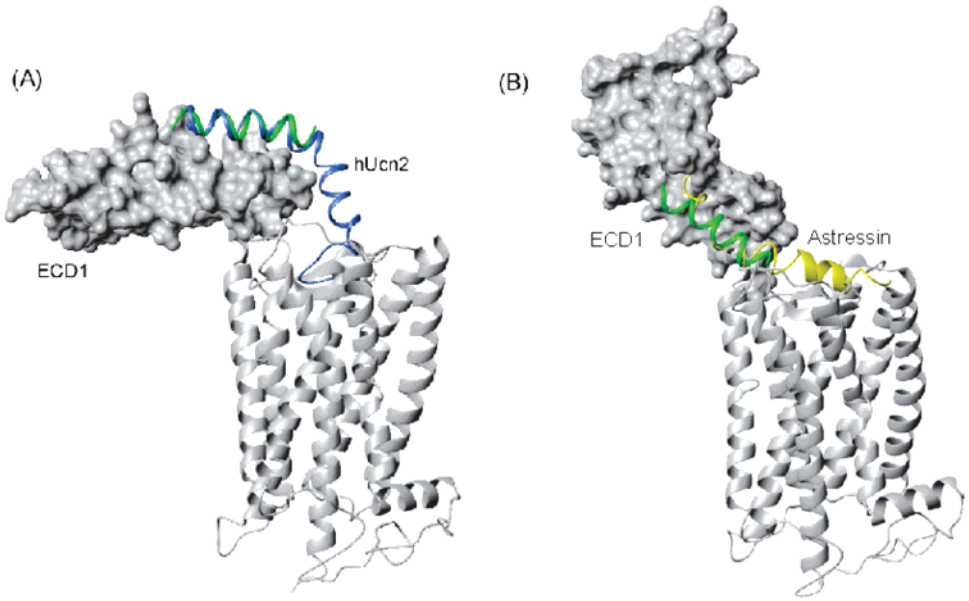

Figure 8. Binding models for the N-terminal binding of CRF family ligands. (A) With the observed kink in the structure of the ligand (hUcn2) shown in blue, the N-terminal of the ligand is in close proximity with the transmembrane region of the receptor (in gray) after the C-terminal binding to the ECD1. (B) Without the kink, the ECD1 has to tilt 90° with respect to its orientation in (A) for the N-terminal of the ligand (shown in yellow) to interact with the juxtamembrane region of the receptor (in gray) after the C-terminal of the ligand binds to the ECD1. Modeling of the transmembrane region is based on the crystal structure of rhodopsin[67] and the NMR structure of the ECD1 in complex with the ligand astressin.[1] ECD1 is placed on the transmembrane region with the $\beta3-\beta4$ segment facing the transmembrane region in A. This orientation is rotated almost 90° about the *y*- and *z*-axes so that the ligand could possibly interact with the juxtamembrane region of the receptor. The ligand shown in green is the C-terminal helix (27−41) of astressin bound to the ECD1 of CRF-R2 receptor shown in gray.[1]

protein.[53] Human CRF and hUcn1 bind to CRF-BP with high affinity, whereas oCRF and astressin do not bind.[54] Residues 6−33 of CRF are important for binding to CRF-BP including, in particular, residues 22, 23, and 25. A comparison of the sequences of human and ovine CRF shows that they differ at positions 22, 23, and 25 in the central domain. The corresponding replacement of residues in oCRF by the corresponding residues from hCRF (i.e., Thr by Ala[22], Lys by Arg[23], and Asp by Glu[25]) enable the mutant oCRF to bind to CRF-BP with high affinity that is comparable to that of hCRF.[54] Similar studies have also been reported for hUcn2, highlighting the importance of residues at 22, 23, and 25 for binding to CRF-BP.[55] In the 3D structures of stressin$_1$ and hUcn1 (Figure 7), these residues are part of the hydrophobic face of the helix, suggesting an interaction with CRF-BP along this hydrophobic face (M. Huising et al. unpublished results).

4. Conclusions

The NMR structures of three CRF analogues with different selectivities, stressin$_1$, astressin B, astressin$_2$-B, and three hormones, hUcn1, hUcn2, and hUcn3, are presented here. In the solvent DMSO, all of these ligands prefer α-helical conformation, with varying degrees of amphipathicity. The C-terminal α-helical conformation observed in most of the free ligands is very similar to the bioactive conformation of astressin bound to the ECD1 of CRF-R2. The ligands that preferred well-defined helical conformation at the C terminus also showed high affinity binding to the ECD1. The amphipathic N-terminal helices could play a crucial role in selectivity of the analogues to CRF-R1, whereas it may not be as important for CRF-R2 binding. The kink between N- and C-terminal helices could also play a crucial role in ligand−receptor interaction. Two binding models are proposed for the CRF family peptide ligand−receptor interaction that requires the kink for the N-terminal interaction of the ligands with the receptor. These models may provide a framework of potential binding mechanisms and shed light onto the variety and complexity of the action of these peptide hormones through different signaling pathways.

5. Experimental Section

5.1. Sample Preparation and NMR Experiments. Analogues were synthesized by the solid-phase approach either manually or on a CS-Bio analogue synthesizer model CS536.[39]

NMR samples were prepared by dissolving 2.5 mg of the analogue in 0.5 mL of DMSO-d_6. The ^{1}H NMR spectra were recorded on a Bruker 700 MHz spectrometer operating at a proton frequency of 700 MHz. Chemical shifts were measured using DMSO (δ = 2.49 ppm) as an internal standard. The 2D spectra were acquired at 293 K. Resonance assignments of the various proton resonances have been carried out using total correlation spectroscopy (TOCSY),[27,28] double-quantum filtered spectroscopy (DQF-COSY),[26] and nuclear Overhauser enhancement spectroscopy (NOESY).[30,56,57] The TOCSY experiments employed the MLEV-17 spin-locking sequence suggested by Davis and Bax,[27] applied for a mixing time of 50 or 70 ms. The NOESY experiments were carried out with a mixing time of 100 or 150 ms. The TOCSY and NOESY spectra were acquired using 800 complex data points in the ω_1 dimension and 1024 complex data points in the ω_2 dimension with t_{1max} = 47 ms and a t_{2max} = 120 ms and were subsequently zero-filled to 1024 × 2048 before Fourier transformation. The DQF-COSY spectra were acquired with 1024 × 4096 data points and were zero-filled to 2048 × 4096 before Fourier transformation. The TOCSY, DQF-COSY, and NOESY spectra were acquired with 16, 16, and 64 scans, respectively, with a relaxation delay of 1 s. The signal from the residual water of the solvent was suppressed using presaturation during the relaxation delay and during the mixing time. The TOCSY and NOESY data were multiplied by 75° shifted sine-function in both dimensions. All spectra were processed using the software PROSA[58] (processing algorithms) and were analyzed using the software X-EASY.[59]

5.2. Structure Determination. The chemical shift assignment of the major conformer was obtained by the standard procedure using DQF-COSY and TOCSY spectra for intraresidual assignment, and the NOESY spectrum was used for the sequential assignment.[32] The collection of structural restraints is based on the NOEs. Dihedral angle constraints were obtained from the intraresidual and sequential NOEs along with the macro GRIDSEARCH in the program CYANA (combined assignment and dynamics algorithm for NMR applications).[60] Calibration of NOE intensities versus ^{1}H−^{1}H distance restraints and appropriate pseudo-atom corrections to the nonstereo specifically assigned methylene, methyl and ring protons were performed using the program CYANA. On an average, approximately 500−600 NOE constraints and 80 angle constraints were utilized while calculating the conformers (Table 3). A total of 100 conformers were initially generated by CYANA, and a bundle containing 20 CYANA conformers with the lowest target function values was utilized for further restrained energy minimization, using the program CNS.[61] The resulting energy-minimized bundle of 20 conformers was used as a basis for discussing the solution conformation of the different analogues. The structures were analyzed using the program PROCHECK[62] and viewed in MOLMOL.[63]

The 3D coordinates of astressin-B, astressin$_2$-B, stressin$_1$, hUcn1, hUcn2, and hUcn3 have been deposited in the protein data bank with the codes 2RMD, 2RM9, 2RME, 2RMF, 2RMG, and 2RMH respectively.

5.2.1. Cloned Receptor-Based Binding Assays. The K_i values given in Table 1 reflect the affinities of the analogues for the various receptors and were derived from competitive radioligand displacement assays using (A) ^{125}I-[Tyr^0,Glu^1,Nle^{17}]-sauvagine and crude membrane fractions from CHO cells stably expressing either CRF-R1α or CRF-R2β[64] or (B) [^{125}I-DTyr^0]-astressin and purified ECD1-CRF-R1 or ECD1-CRF-R2β.[65,66] The K_i values were determined by computer program

(53) Linton, E. A.; Perkins, A. V.; Woods, R. J.; Eben, F.; Wolfe, C. D. A.; Behan, D. P.; Potter, E.; Vale, W. W.; Lowry, P. J. *J. Clin. Endocrinol. Metab.* **1993**, *76*, 260−262.
(54) Sutton, S. W.; Behan, D. P.; Lahrichi, S.; Kaiser, R.; Corrigan, A.; Lowry, P.; Potter, E.; Perrin, M.; Rivier, J.; Vale, W. W. *Endocrinology* **1995**, *136*, 1097−1102.
(55) Isfort, R. J.; Wang, F.; Tscheiner, M.; Dolan, E.; Bauer, M. B.; Lefever, F.; Reichart, D.; Wehmeyer, K. R.; Reilman, R. A.; Keck, B. D.; Hinkle, R. T.; Mazur, A. W. *Peptides* **2006**, *27*, 1806−1813.
(56) Macura, S.; Ernst, R. R. *Mol. Phys.* **1980**, *41*, 95−117.
(57) Macura, S.; Huang, Y.; Suter, D.; Ernst, R. R. *J. Magn. Reson.* **1981**, *43*, 259−281.
(58) Güntert, P.; Dotsch, V.; Wider, G.; Wüthrich, K. *J. Biolmol. NMR* **1992**, *2*, 619−629.
(59) Eccles, C.; Güntert, P.; Billeter, M.; Wüthrich, K. *J. Biomol. NMR* **1991**, *1*, 111−130.
(60) Güntert, P.; Mumenthaler, C.; Wüthrich, K. *J. Mol. Biol.* **1997**, *273*, 283−298.
(61) Brunger, A. T.; Adams, P. D.; Clore, G. M.; Delano, W. L.; Gros, P.; Grosse-Kunstleve, R. W.; Jiang, J. S.; Kuszewski, J.; Nilges, M.; Pannu, N. S.; Read, R. J.; Rice, L. M.; Simonson, T.; Warren, G. L. *Acta Crystallogr., Sect. D.* **1998**, *54*, 905−921.
(62) Laskowski, R. A.; MacArthur, M. W.; Moss, D. S.; Thornton, J. M. *J. Appl. Crystallogr.* **1993**, *26*, 283−291.
(63) Koradi, R.; Billeter, M. *PDB Newsletter* **1998**, *84*, 5−7.
(64) Perrin, M. H.; Sutton, S. W.; Cervini, L.; Rivier, J. E.; Vale, W. W. *J. Pharmacol. Exper. Ther.* **1999**, *288*, 729−734.
(65) Perrin, M. H.; DiGruccio, M. R.; Koerber, S. C.; Rivier, J. E.; Kunitake, K. S.; Bain, D. L.; Fischer, W. H.; Vale, W. W. *J. Biol. Chem.* **2003**, *278*, 15595−15600.
(66) Perrin, M. H.; Fischer, W. H.; Kunitake, K. S.; Craig, A. G.; Koerber, S. C.; Cervini, L. A.; Rivier, J. E.; Groppe, J. C.; Greenwald, J.; Nielsen, S. M.; Vale, W. W. *J. Biol. Chem.* **2001**, *276*, 31528−31534.
(67) Palczewski, K.; Kumasaka, T.; Hori, T.; Behnke, C. A.; Motoshima, H.; Fox, B. A.; Trong, I. L.; Teller, D. C.; Okada, T.; Stenkamp, R. E.; Yamamoto, M.; Miyano, M. *Science* **2000**, *289*, 739−745.

GraphPad Prism program (GraphPad Softwares, Inc., San Diego CA). All assays were performed in triplicate at least three times.

Acknowledgment. This work was supported in part by NIH Grant DK026741 and the Clayton Medical Research Foundation, Inc. We thank Dr. W. Fisher and W. Low for mass spectrometric analyses, Dr. Gulyas, L. Cervini, R. Kaiser, J. Vaughan, and C. Miller for technical assistance in the synthesis and chemical and biological characterization of peptides. We are indebted to D. Doan for manuscript preparation. J.E.R. is the Dr. Frederik Paulsen Chair in Neurosciences. W.W.V. is the Helen McLoraine Professor of Molecular Neurobiology and an FMR Senior Investigator. We thank the H. and J. Weinberg Foundation, the H.N. and F.C. Berger Foundation, and the Auen Foundation for financial support. R.R. is the Pioneer Fund Development Chair.

Supporting Information Available: Chemical shifts of various protons in DMSO-d_6 for astressin B, astressin$_2$-B, and stressin$_1$; chemical shift assignments of various proton resonances in human urocortins 1, 2, and 3. This material is available free of charge via the Internet at http://pubs.acs.org.

JA0760933